Perturbation of Nanoparticle on Deformed Microcavity

Qinghai Song and Young L. Kim

***Abstract*—Here we studied the perturbation of nanoparticles on the resonances in deformed microcavities. Owing to the breaking of rotational symmetry in deformed cavities, the field distributions are not uniform along the cavity boundary and thus result in position dependent perturbation of a single scatterer. Combined with the directional emission of deformed cavities, such perturbation provides the possibility to detect the position of nanoparticle in the far field. Our numerical example shows that a position change of the nanoparticle in 100 nm on the boundary can induce a spectral shift of $\sim$0.02 nm, which can be easily resolved by a conventional spectrometer.**

***Index Terms*—Chaotic, microcavity, perturbation.**

I. Introduction

WHISPERING GALLERY MODES (WGM) based microcavities have been the object of intensive investigation for several important applications including nanophotonics circuits, integrated optical chips, and optical communications [1], [2]. Recently, such microcavities have been proposed as a powerful method to achieve sensitive sensors because of their ultrahigh Q factors [3]. It was experimentally demonstrated that the highest Q factor in microspheres can be as high as 8×10^9 [4], which in turn provides the ultrahigh sensitivity for detecting single molecules using a resonant wavelength shift [5]–[9]. A recent experimental study [10] has demonstrated that perturbation caused by mode splitting in a microcavity can be used as a highly accurate method for measuring single nanoparticle sizes, based on a model from single particle perturbation [11]. However, due to the rotational symmetry of circular microcavities, these techniques are not sensitive to the position of the scatterer. The applications are also limited by nanoscale manipulation of the fiber or waveguide position [4]–[10]. Here, we studied the perturbation of a nanoparticle on the resonances in deformed microcavities. High Q modes and scar modes in deformed microcavities show high sensitivity of perturbation to a particle position. The combination of position dependent perturbation and directional emission of deformed microcavities can open a new possibility to detect signals of a single particle or molecule in the far field. Our numerical example shows the position sensitivity in spectrum can be as high as 0.0178 nm when the binding site of the nanoparticle is changed for 100 nm, which is easily resolved using common spectrometers.

Manuscript received April 19, 2010; revised July 07, 2010; accepted August 03, 2010. Date of publication August 16, 2010; date of current version September 10, 2010. This work was supported in part by a grant from Purdue Research Foundation.

The authors are with the Weldon School of Biomedical Engineering, Purdue University, West Lafayette, IN 47907 USA (e-mail: qinghai.song@gmail.com).

Color versions of one or more of the figures in this paper are available online at http://ieeexplore.ieee.org.

Digital Object Identifier 10.1109/JLT.2010.2066259

II. Theoretical Analysis

When a nanoparticle is placed on the boundary of a microcavity, the degenerated clockwise (CW) and counter clockwise (CCW) modes are lifted and coupled each other [12], [13]. Thus, we need to take into account the amplitude of the CW and CCW modes together to describe the scattering effect of the nanoparticle. In this case, the perturbation on resonant fields should be proportional to $f^2(r)$, where f(r) is the field distribution on the boundary [11]. In a circular cavity, due to the rotational symmetry, the field is uniformly distributed along the boundary. Thus, neither spectra shift nor mode splitting is sensitive to the particle position. On the other hand, in a deformed microcavity, the breaking of rotational symmetry of the cavity shape also breaks the uniform field distribution along the cavity boundary and therefore enables the position dependence of perturbation.

This can be easily understood with a simple ray model. Fig. 1(a) shows the total internal reflection confined WGM in a circular cavity. The Poincare surface of section (SOS) is illustrated in Fig. 1(b), where S and $\mathrm{Sin}\chi$ correspond to the arclength coordinate along the circumference and the light incident angle of the total internal reflection, respectively. The blue line, which can be a simple analogy to the field distribution of the resonant mode, is found to be invariable along the cavity boundary. However, in a deformed microcavity, the straight line is distorted to curves, broken curves, islands, and finally chaotic sea [14]–[16]. In an example of a limacon cavity (in the polar coordinate, $\rho = \mathrm{R}(1 + \varepsilon \cos\theta)$ with $\varepsilon = 0.35$, where R is the radius and ε is the deformation parameter), the trajectory are focused on several bouncing points (points 1–4) only on the cavity boundary in Fig. 1(c) and (d). Therefore, the final field distribution is focused on around these points on the cavity boundary, allowing the sensitivity to the scatterer's position.

III. Numerical Simulation

We systematically tested our concept using a finite element method (COMSOL Multiphysics 3.5a). We kept the limacon shape as $\rho = \mathrm{R}(1 + \varepsilon \cos\theta)$ with $\varepsilon = 0.35$ because it can provide ultrahigh Q factors and totally break the continuous field distribution along the cavity boundary [17]. Compared with high Q quadruple cavity ($\rho = \mathrm{R}(1 + \varepsilon \cos 2\theta)$ with $\varepsilon < 0.06$), this almost full chaotic cavity can provide more dramatic shape sensitivity. Meanwhile, the unidirectional emission from such a cavity can also enable the far field detection [17]–[21]. For simplicity, we reduced our system to a two-dimensional structure and the polarization is limited to TE (E in plane). The

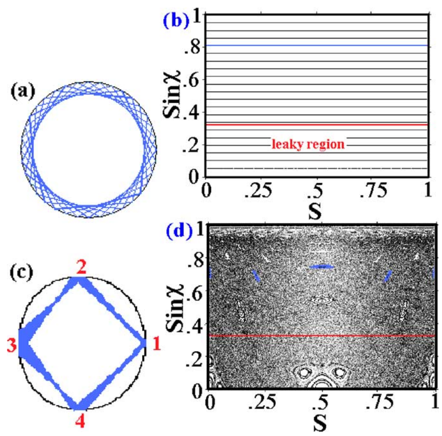

Fig. 1. (a) WGM trajectory in a circular microcavity. (b) Poincare SOS showing the trajectory (blue line) in phase space. (c) Diamond trajectory in a limacon shaped microcavity. (d) Poincare SOS for the trajectory (blue dots) in phase space, where chaotic sea can be observed. The solid lines in (b) and (c) represent their ray orbits.

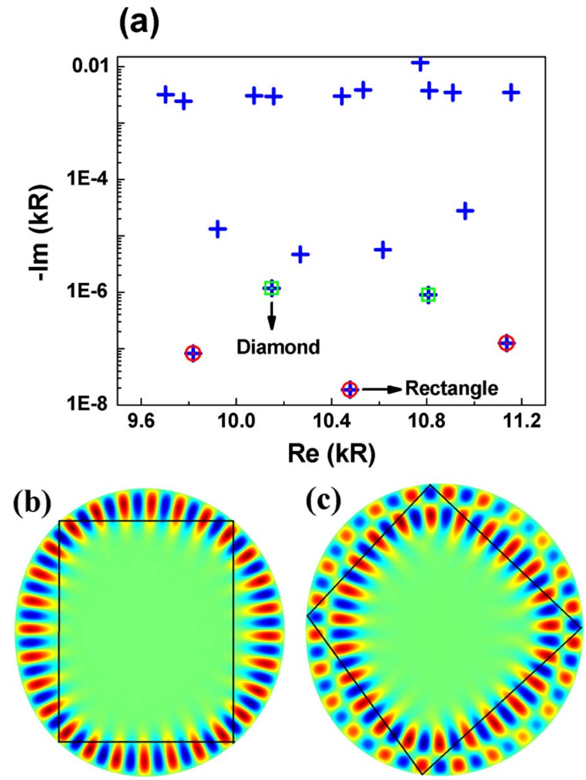

Fig. 2. (a) Eigenvalues in the limacon shaped microcavity. Two types of high Q factors resonant modes are marked with the red open circles and the green open squares. The Q factor is defined as $\mathrm{Re(kR)}/2/|\mathrm{Im}(kR)|$. (b) and (c) show the corresponding mode distribution (Hz) of the two resonant modes marked by the arrows in (a). The black solid lines show the corresponding orbits.

refractive index of the microcavity is 3.13, which is defined by the effective refractive index of GaAs [18].

We first calculated the eigenvalues and Fig. 2(a) shows the plot of $-\mathrm{Im(kR)}$ vs Re(kR), where k is the wavevector in vacuum $(\mathrm{k} = 2\pi/\lambda)$ and R is radius of the cavity. As shown in in Fig. 2(a), several types of high Q modes can be observed. The red circles represent rectangle series of high Q modes, which are confined by wave localization [22] on the rectangle unstable periodic orbits (UPO) [14]. The Q factor obtained from such modes is greater than 10^8. The corresponding field distribution is shown in Fig. 2(b), where the black solid lines show the UPO. Another type of high Q modes is marked as the green squares in Fig. 2(a). Their Q factors are slightly lower than those of the rectangle orbit modes, but still higher than 10^6. The corresponding field distribution and orbits are shown in Fig. 2(c). Hereafter, this kind of mode is referred to as a diamond mode. These two types of the resonant modes have the highest Q factors and are most possible candidates to lase as active biosensors [8].

To test the binding-site dependence of this deformed cavity, we placed a nanoparticle with a radius of 50 nm on the cavity boundary, as shown in the inset of Fig. 3(a). First, we studied the rectangle mode, which is marked by the black arrow in Fig. 2(a). The Q factor is greater than 2.8×10^8, which is as high as those of most circular cavities, promising an ultrahigh sensitivity. After the nanoparticle is attached onto the cavity, the resonant mode will split into symmetric and anti-symmetric modes, which have node or anti-node at the particle position (Insets in Fig. 3(b)). Fig. 3(a) shows the position dependence of mode splitting on the position of the scatterer. As the limacon shape has mirror symmetry along $\theta = 0$, we only studied the S from 0 to 0.5. The mode splitting varies with the scatterer position and two peaks can be observed. The similar behavior of the spectra shift is shown in Fig. 3(b). Two modes shift to longer wavelengths together because of the increase in the refractive index or the radius [3]. Meanwhile, the wavelength shifts are also dependent on the position. Two maximum points can be observed at the same S positions in Fig. 3(a). To confirm the relationship between the spectra shift and the mode splitting, we plotted $\mathrm{f}^2(\mathrm{r})$ of the rectangle mode along the perimeter in Fig. 3(c). We found that the behaviors of the mode splitting and the resonant wavelengths are qualitatively consistent with $\mathrm{f}^2(\mathrm{r})$. Both the position dependence and peak positions are very similar. The slight difference can be caused by the effective mode volume, cavity loss channel, and absolute amplitude of the field.

We further tested our concept with the mode splitting and wavelength shift of the resonant modes along the diamond orbit in Fig. 2(d). Results from our numerical simulations show that both mode splitting (Fig. 4(a)) and spectra shift (Fig. 4(b)) of the diamond mode are also dependent on the position of the scatterer, similarly to Fig. 3. The only difference is that their maximum points follow the maximum field distribution of the diamond orbit, where the maximum points are around $\theta \sim 0, 180, 90$, and 270, respectively (Fig. 4(c)).

The analysis and numerical simulation above show the position dependence of perturbation in the deformed microcavity. In other words, the same nanoparticle will generate different spectra shift or mode splitting when it binds to a different location on the cavity boundary. Thus this kind of mechanism could potentially be used to detect the position of nanoparticles. For example, from $\mathrm{S} = 0.25$ to $\mathrm{S} = 0.339$ in Fig. 3(b), every 100-nm position shift can generate a spectral change in about 0.0178 nm, which is large enough for most spectrometers

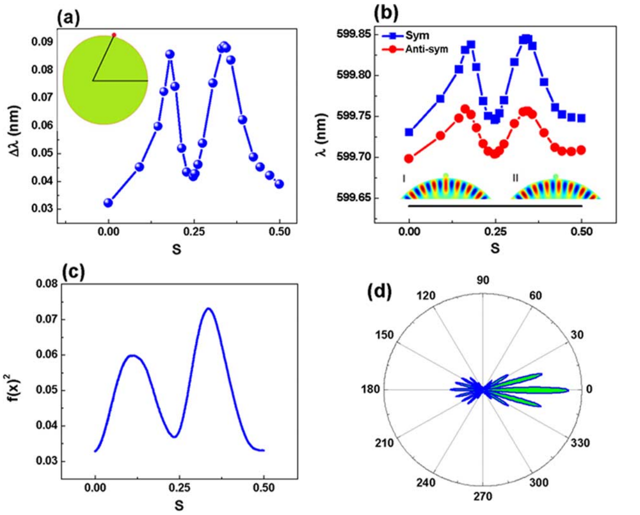

Fig. 3. (a) Mode splitting (b) resonant wavelengths and (c) square of the field distribution versus the position of the scatter for the rectangle resonant mode. The solid line in (b) is the wavelength position of a bare cavity. Strong position dependence can be observed. Sym and Anti-sym denote original symmetric and anti-symmetric modes. The spatial resolution is 0.0178 nm/100 nm. 0.0178 nm can be well resolved by general laser spectrum. (d) is the corresponding far field pattern. Unidirectional emission can be observed. Inset in (a): Schematic picture of a limacon cavity based biosensor. Inset in (b): Field patterns of symmetric and anti-symmetric around the nanoparticles.

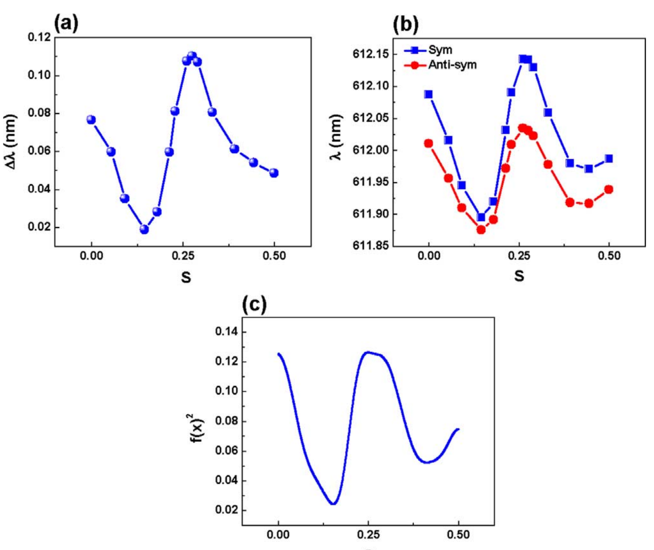

Fig. 4. (a) Mode splitting, (b) resonant wavelengths, and (c) square of the field distribution versus the position of the scatter for the diamond resonant mode.

[18]. Moreover, the deformed microcavity has a unique property-directional emission. In an active microcavity, this property enables the detection in the far field. Fig. 3(d) shows the far field patterns of the highest Q resonant mode on the rectangle orbit. Similar to our previous report, an obvious unidirectional emission can be observed along $\theta = 0$ [18]. As the emission light is confined in a narrow angle range, the slight near field perturbation can be easily detected in the far field without a further precise controlled fiber or waveguide coupler. It should be noted that the position sensitivity of perturbation can be more dramatic if a larger cavity is applied and the resonances are away from the crossing/anti-crossing points [23], [24]. This is because the physical size of scar modes on the boundary (spot size in phase space) is proportional by the effective Planck constant ($\sim 1/\mathrm{nkR}$).

Furthermore, in a circular microcavity, as the CW and CCW modes overlap in real space, the perturbation of the field distribution in the CW and CCW modes are the same. On the other hand, in a deformed microcavity, because of the Goos-Hanchen shift that must be considered in small cavities, the CW and CCW modes shift in the opposite direction and are not exactly overlapped in real space, especially at the maximum field positions of the bouncing points [25]. In this case, the perturbation of the scatterer at one point is not equal for the CW and CCW modes. If the CW and CCW modes are not real degenerated, four eigenvalues should be obtained. However, the final eigenvalues of superposition are only two in our simulation. This directly proves that the CW and CCW modes in our deformed cavity are indeed degenerated modes.

In summary, we have studied the perturbation of nanoparticle on the resonances in the deformed microcavity. We found that both mode splitting and the wavelengths of symmetric and anti-symmetric modes are dependent on the location of a nanoparticle on the cavity boundary. This is because of the un-uniform field distribution in the deformed cavity, which is formed by rotational symmetry breaking. Combined with the directional emission of the deformed cavity, such perturbation can be potentially used to detect the location of a nanoparticle in the far field.

REFERENCES

[1] *Optical Processes in Microcavities*, ser. Advanced Series in Applied Physics, R. K. Chang and A. M. Campillo, Eds.. Singapore: World Scientific, 1996.

[2] , K. J. Vahala, Ed., *Optical Microcavities*, ser. Advanced Series in Applied Physics. Singapore: World Scientific, 2004.

[3] F. Vollmer and S. Arnold, "Whispering-gallery-mode biosensing: label-free detection down to single molecules," *Nature Method*, vol. 5, pp. 591–596, 2008.

[4] M. L. Gorodetsky, A. A. Savchenkov, and V. S. Ilchenko, "Ultimate Q of optical microsphere resonators," *Opt. Lett.*, vol. 21, p. 453, 1996.

[5] F. Vollmer, D. Braun, A. Libchaber, M. Khoshsima, I. Teraoka, and S. Arnold, "Protein detection by optical shift of a resonant microcavity," *Appl. Phys. Lett.*, vol. 80, pp. 4057–4059, 2002.

[6] E. Krioukov, D. J. W. Klunder, A. Driessen, J. Greve, and C. Otto, "Sensor based on an integrated optical microcavity," *Opt. Lett.*, vol. 27, pp. 512–514, 2002.

[7] S. Arnold, M. Khoshsima, I. Teraoka, S. Holler, and F. Vollmer, "Shift of whispering-gallery modes in microspheres by protein adsorption," *Opt. Lett.*, vol. 28, pp. 272–274, 2003.

[8] H. Li, L. Shang, X. Tu, L. Y. Liu, and L. Xu, "Coupling variation induced ultrasensitive label free bio-sensing by using single mode coupled microcavity laser," *J. Am. Chem. Soc.*, vol. 131, p. 16612, 2009.

[9] A. M. Armani, R. P. Kulkarni, S. E. Fraser, R. C. Flagan, and K. J. Vahala, "Label-free, single molecule detection with optical microcavities," *Science*, vol. 317, pp. 783–787, 2007.

[10] J. G. Zhu, S. K. Ozdemir, Y. F. Xiao, L. Li, L. N. He, D. R. Chen, and L. Yang, "On-chip single nanoparticle detection and sizing by mode splitting in an ultrahigh-Q microresonator," *Nature Photon*, vol. 4, pp. 46–49, 2010.

[11] A. Mazzei, S. Götzinger, L. de S. Menezes, G. Zumofen, O. Benson, and V. Sandoghdar, "Controlled coupling of counterpropagating whispering-gallery modes by a single Rayleigh scatterer: a classical problem in a quantum optical light," *Phys. Rev. Lett.*, vol. 99, p. 173603, 2007.

[12] T. J. Kippenberg, A. L. Tchebotareva, J. Kalkman, A. Polman, and K. J. Vahala, "Purcell-factor-enhanced scattering from Si nanocrystals in an optical microcavity," *Phys. Rev. Lett.*, vol. 103, p. 027406, 2009.

[13] M. L. Gorodetsky, A. D. Pryamikov, and V. S. Ilchenko, "Rayleigh scattering in high-Q microspheres,," *J. Opt. Soc. Am. B*, vol. 17, pp. 1051–1057, 2000.
[14] J. U. Nockel and A. D. Stone, "Ray and wave chaos in asymmetric resonant optical cavities," *Nature*, vol. 385, pp. 45–47, 1997.
[15] C. Gmachl, F. Capasso, E. E. Narimanov, J. U. Nockel, A. D. Stone, J. Faist, D. L. Sivco, and A. Y. Cho, "High-power directional emission from microlasers with chaotic resonators," *Science*, vol. 280, pp. 1556–1564, 1998.
[16] J. U. Nockel, A. D. Stone, and R. K. Chang, "Q-spoiling and directionalities in deformed ring cavities," *Opt. Lett.*, vol. 19, pp. 1693–1695, 1994.
[17] J. Wiersig and M. Hentschel, "Combining directional light output and ultralow loss in deformed microdisks," *Phys. Rev. Lett.*, vol. 100, p. 033901, 2008.
[18] Q. H. Song, W. Fang, B. Y. Liu, S. T. Ho, G. S. Solomon, and H. Cao, "Chaotic microcavity laser with high quality factor and unidirectional output," *Phys. Rev. A*, vol. 80, p. 041807®, 2009.
[19] C. L. Yan, Q. J. Wang, L. Diehl, M. Hentschel, J. Wiersig, N. F. Yu, C. Pflugl, F. Capasso, M. A. Belkin, T. Edamura, M. Yamanishi, and H. Kan, "Directional emission and universal far-field behavior from semiconductor lasers with limaccedilon-shaped microcavity," *Appl. Phys. Lett.*, vol. 94, p. 251101, 2009.
[20] S. Shinohara, M. Hentschel, J. Wiersig, T. Sasaki, and T. Harayama, "Ray-wave correspondence in limacon-shaped semiconductor microcavities," *Phys. Rev. A*, vol. 80, p. 031801®, 2009.
[21] C. H. Yi, M. W. Kim, and C. M. Kim, "Lasing characteristics of a Limacon-shaped microcavity laser," *Appl. Phys. Lett.*, vol. 95, p. 141107, 2009.
[22] V. A. Podolsky, E. Narimanov, W. Fang, and H. Cao, "Chaotic microlasers based on dynamical localization," *Proc. Nat. Acad. Sci.* , vol. 101, pp. 10498–10500, 2004.
[23] J. Wiersig, "Formation of long-lived, scarlike modes near avoided resonance crossings in optical microcavities," *Phys. Rev. Lett.*, vol. 97, p. 253901, 2006.
[24] Q. H. Song and H. Cao, "Improving optical confinement in nanostructures via external mode coupling," *Phys. Rev. Lett.*, vol. 105, p. 253901, 2009.
[25] J. Unterhinninghofen, J. Wiersig, and M. Hentschel, "Goos-Hanchen shift and localization of optical modes in deformed microcavities," *Phys. Rev. E*, vol. 78, p. 016201, 2008.

Qinghai Song received the B.S. and Ph.D. degrees from Fudan University, Shanghai, China.

His main research interests are the light confinements in microcavities, nanocavities, and disordered materials, which include designing, fabricating, and characterization of semiconductor and polymer microdisk, Surface plasmon and nanorod based nanocavity and random lasers in disordered materials.

Young L. Kim received the Ph.D. degree in biomedical engineering from Northwestern University, Evanston, IL.

His research interests are in understanding light propagation in random media such as biological tissue, developing advanced biophotonics techniques, and further translating these techniques to clinical settings.